Organometallic Nonlinear Optical Polymers. 4. Organometallic Main-Chain, Side-Chain, and Guest-Host Polymers: A Study of Their Orientation and Relaxation Using Second Harmonic Generation

Michael E. Wright* and Edward G. Toplikar

Department of Chemistry and Biochemistry, Utah State University, Logan, Utah 84322-0300

Hilary S. Lackritz* and John T. Kerney

School of Chemical Engineering, Purdue University, West Lafayette, Indiana 47907-1283

Received November 30, 1993; Revised Manuscript Received February 9, 1994®

ABSTRACT: In this paper several new organometallic polymers have been prepared. Structure-property relationships for local polymer mobility and the net orientation of the organometallic nonlinear optical (NLO)-phores have been investigated using second harmonic generation (SHG). The methacrylate organometallic derivatives $\{\eta^5\text{-}C_5H_4CH_2O_2CC(CH_3)=CH_2\}Fe\{\eta^5\text{-}C_5H_4CH=C(CN)X\}$ [**4a**, X = *p*-C_6H_5Br; **4b**, X = 4-pyridyl; **4c**, X = CN; **4d**, X = CO_2Et] and $\{\eta^5\text{-}C_5H_4CH=C(CN)CO_2(CH_2)_2O_2CC(CH_3)=CH_2\}Fe\{\eta^5\text{-}C_5H_5\}$ (**7**) were prepared and polymerized with methyl methacrylate (5/95, mol/mol) to afford copolymers **8a-d** and **9**, respectively. Comonomer $\{\eta^5\text{-}C_5H_4CH=C(CN)CO_2(CH_2)_2OH\}Fe\{\eta^5\text{-}C_5H_4CH_2OH\}$ (**5**) was synthesized and reacted with 1,6-diisocyanatohexane to yield a main-chain NLO organometallic polyurethane **10** (M_n = 7600, T_m = 176 °C). In addition, a poly(methyl methacrylate) guest-host film of NLO-phore **5** was prepared. Corona poling and SHG measurements were made under a variety of carefully controlled experimental conditions. In the case of the covalently bound ferrocenyl NLO-phore, temporal stability was greatest for the smaller acceptor group CH=$C(CN)_2$ (*i.e.*, copolymer **8c**). The rate of relaxation for copolymer **8d** was faster than that for **9**, indicating that the point of attachment on the ferrocenyl NLO-phore to the polymer backbone was an important consideration. It was found that physically aging the organometallic polymers prior to poling produced samples which displayed a smaller initial SHG signal; however, the signal was significantly more stable for a longer time. The guest-host system using NLO-phore **5**, with its multiple hydrogen-bonding sites, was observed to have very good long-term temporal stability. The guest-host polymer was poled negatively and showed enhanced temporal stability in comparison to a positively poled sample. The organometallic main-chain copolymer **10** responded well to poling but had concomitant decomposition, leading to an underestimation of orientational stability.

Introduction

Organometallic complexes with nonlinear optical (NLO) properties represent an interesting and potentially useful category of substances which bridge the well-known areas of inorganic[1] and organic NLO substances.[2] Although there are many organometallic complexes which have $\chi^{(2)}$ NLO properties,[3] ferrocene derivatives have been shown experimentally[4] and theoretically[5] to be one of the most efficient. Furthermore, attractive NLO properties are coupled with excellent thermal (500 °C) and photochemical stability.[6] These properties combine to make ferrocene compounds a unique class of organometallic NLO materials. In this study we continue to explore the synthesis of new organometallic NLO materials based on polymeric ferrocene derivatives.[7] A systematic investigation covering the orientation by poling and the resulting temporal stabiiity of ferrocene NLO-phores has been conducted using NLO techniques.

To observe frequency doubling, the nonlinear optical dopants (NLO-phores) must be oriented noncentrosymmetrically, which is generally accomplished by applying an electric field. The electric field induced orientation can only occur in regions of sufficient local mobility. By making small structural changes on the NLO-phore, the local environment is altered and hence the ability of the NLO-phore to orient is changed. Thus, second harmonic generation (SHG) provides an excellent technique for probing the molecular environment of the polymer matrix in close proximity to the NLO-phore. Disorientation of the NLO-phores occurs due to segmental mobility of the polymer. Electric field effects could also contribute to the decay of the optical signal and must be considered. Thus, by monitoring the stability of the optical signal with SHG and hence the polymeric microenvironment, information concerning the orientation of the NLO-phore may be gained, and a structure-property relationship between local polymer mobility and net dipole orientation may be established. This type of analysis has not been performed on organometallic NLO-phores until this study.

The Williams-Watts (WW) stretched exponential given by $y = A \exp[(-t/\tau)^\beta]$ has been traditionally used to describe polymer relaxation behavior below the glass transition (T_g) temperature.[8] Previous studies have attempted to use this relation to fit the decay of the second-order macroscopic susceptibility following the removal of an applied electric field for guest-host systems[9] and more recently for side-chain NLO polymers;[10] it was found that in both studies this equation did not completely describe the polymer relaxation behavior. In this investigation, the organometallic side-chain NLO polymers are even more complex, and it is shown that the WW equation does not accurately describe relaxation phenomena occurring in these systems.

Results and Discussion

Organometallic NLO Monomer and Polymer Syntheses. We recently described the synthesis of complex

® Abstract published in *Advance ACS Abstracts*, March 15, 1994.

0024-9297/94/2227-3016$04.50/0

Scheme 1

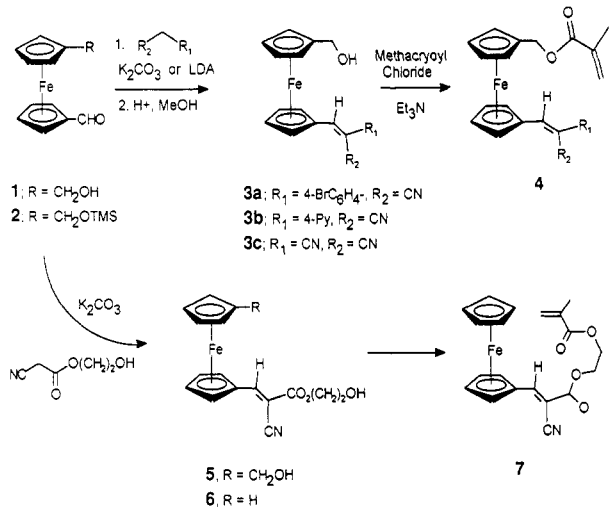

1 based on the sequential transmetalation of the readily available 1,1'-bis(tributylstannyl)ferrocene.[11] Complex 1 serves as an excellent starting point for the synthesis of unsymmetrically functionalized ferrocene monomers.[12] The carboxaldehyde moiety undergoes base-assisted (lithium diisopropylamide (LDA) or K_2CO_3) condensation reactions with active methylene compounds. When using the stronger base LDA for the preparation of **3a** and **3b**, it is found that protection of the alcohol group as the trimethylsilyl ether (**2**) provides a significant improvement in conversion efficiency. Treatment of the alcohol functional group with methacryloyl chloride in the presence of triethylamine affords the methacrylate monomers **4a–c** in good overall yield (Scheme 1). Condensation of $NCCH_2CO_2(CH_2)_2OH$ (prepared from cyanoacetic acid and ethylene glycol/DCC coupling) with **1** and ferrocene carboxaldehyde afforded compounds **5** and **6**, respectively. Subsequent treatment of **6** with methacryloyl chloride affords monomer **7** in reasonable yield.

The methacrylate monomers **4a–c** and **7** were copolymerized with methyl methacrylate in benzene using free-radical initiation (AIBN) at a temperature of 80 °C over a 6-h period. A monomer ratio of 95/5 (methyl methacrylate/ferrocene monomer, mol/mol) is used for the polymerization reactions. The polymerization mixtures remained homogeneous with the exception of polymer **8c**.

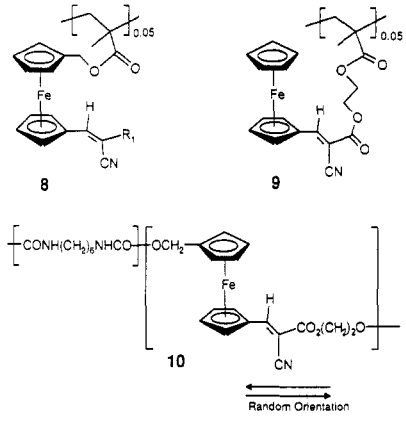

A significant fraction of polymer **8c** precipitated from the solution and did not redissolve after the initial precipitation in methanol. This is perhaps best explained by cross-linking occurring through the very reactive α,α-dicyanoethylene unit. The polymers reported in Table 1 have been purified by redissolving the crude material in chloroform, filtering, and then reprecipitating in methanol.

Table 1. Molecular Weights and T_g Data for Polymers 8–10

copolymer	M_n	T_g (°C)	T_m (°C)
8a	30 000	112	
8b	21 000		
8c	13 000	110	
9	43 000	100	211
10	7 600		176

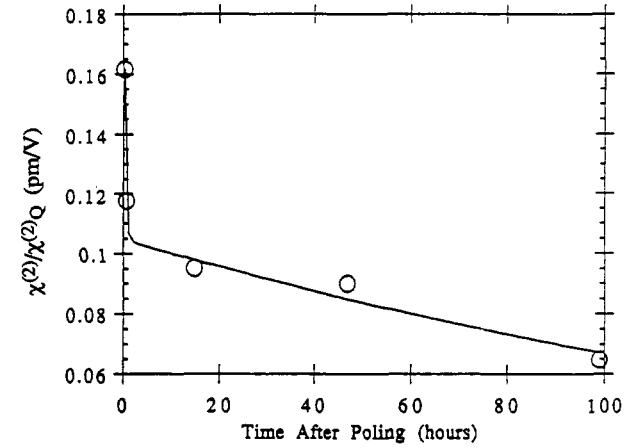

Figure 1. Long-term stability of $\chi^{(2)}/\chi^{(2)}_Q$ for copolymer **8c**. The solid line indicates a biexponential fit with fitting parameters $\theta_1 = 0.11$, $\tau_1 = 0.32$ h; $\theta_2 = 0.10$, $\tau_2 = 225$ h.

This procedure is repeated at least three times. The polymers are all well characterized by proton NMR spectroscopy, UV–vis, and elemental analysis data. All data confirm the incorporation of the intact NLO-phore and at the same mole percent as the initial monomer ratio (95/5). Molecular weight data for each polymer are determined by GPC versus polystyrene standards (Table 1).

Preparation of copolymer **10** is carried out by treatment of complex **5** with 1,6-diisocyanatohexane in refluxing dioxane for 10 h. Polymer formation is monitored by GPC analysis, and the results presented represent an optimized polymerization time and temperature. The organometallic polyurethane is precipitated in methanol and purified by washing with methanol. The polymer could be obtained in modest yield, showing no apparent T_g but rather a T_m. The latter event is erased after the first DSC scan and is a product of the precipitation process.

Orientation and Relaxation Studies Using SHG. Initial experiments were conducted to determine the optimum conditions for observing SHG for side-chain polymers **8** and **9**. Only copolymer **8b** did not show any SHG activity after corona poling at T_g + 25 °C. Polymers **8a** and **8c** displayed the highest SHG signals when poling temperatures of T_g + 25 °C are employed. In this temperature region the polymer is mobile enough to allow the NLO-phores to readily orient into the required noncentrosymmetric macroscopic structure, yet the temperature is generally not sufficiently excessive to degrade the polymer or have electric field effects dominate.[13] It is also important to note that second-order susceptibility is inversely proportional to temperature.[14]

The polymers are poled at T_g + 25 °C for 20 min and then allowed to cool to ambient temperature with the electric field still applied. Upon reaching ambient temperature, the voltage is removed, and decay of the SHG signal is monitored. The decay of $\chi^{(2)}$ over time for **8a** and **8c** is shown in Figures 1 and 2, respectively. The decay data following the removal of the electric field was not successfully fit using the Williams–Watt stretched expo-

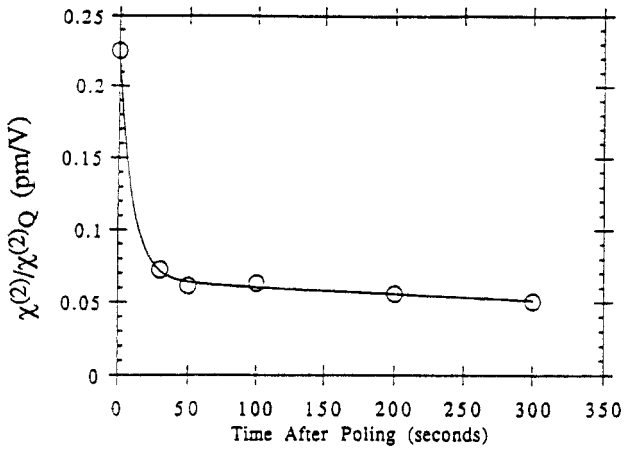

Figure 2. Long-term stability of $\chi^{(2)}/\chi^{(2)}_Q$ for copolymer **8a**. The solid line indicates a biexponential fit with fitting parameters $\theta_1 = 0.16$, $\tau_1 = 10$ s; $\theta_2 = 0.07$, $\tau_2 = 1231$ s.

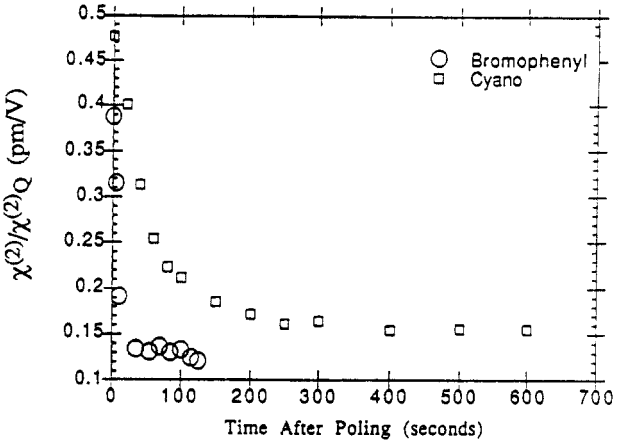

Figure 3. Stability of $\chi^{(2)}/\chi^{(2)}_Q$ for copolymers **8a** (○) and **8c** (□) following erasure of thermal history.

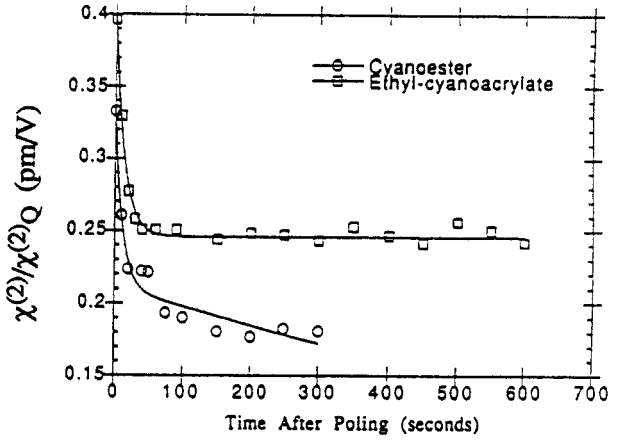

Figure 4. Decay of $\chi^{(2)}/\chi^{(2)}_Q$ following corona poling for copolymers **9** (○) and **8d** (□). The solid line indicates a biexponential fit for each system. For copolymer **8d** the fitting parameters are $\theta_1 = 0.15$, $\tau_1 = 14$ s; $\theta_2 = 0.25$, $\tau_2 = 10^{12}$ s and $\theta_1 = 0.12$, $\tau_1 = 11$ s; $\theta_2 = 0.21$, $\tau_2 = 1453$ s for copolymer **9**.

nential. The WW fit predicted a slower decay than that experimentally observed at short times and predicted a faster decay than that experimentally observed at long times. An alternative biexponential fit, $y = \theta_1 \exp(-t/\tau_1) + \theta_2 \exp(-t/\tau_2)$, was used to fit the data and is represented as a solid line in the figures. This equation is based on fitting parameters which do not have direct physical significance for describing relaxation behavior but can be used to illustrate a "short-time" and "long-time" relaxation. Charge distribution and third-order effects are important in all poled polymer systems. Data published by Boyd *et al.*[16] and Torkelson *et al.*[13,16] indicate that the contribution of these effects is often less than 10% and occur in very short time scales. This will possibly contribute to the inability of the stretched exponential type equation to fit the data well. The WW fit has been successfully used to describe decays in contact poled films.[17]

It appears that packing of the polymer chains is the dominant effect in the orientation and relaxation behavior of the organometallic NLO-phore. Packing appears to be dependent not only upon NLO-phore structure but also on the age of the polymer films. Interestingly, the smaller NLO-phore (*i.e.*, in **8c**) shows a lower initial SHG signal; however, it shows a better long-term stability in comparison to the larger NLO-phore in **8a**. Polymer **8c** exhibits an observable signal for hours as opposed to seconds (Figures 1 and 2). This marked difference in behavior of $\chi^{(2)}$ for the two systems may be rationalized with molecular packing arguments. The polymer chains which pack more efficiently may provide a more stable microenvironment for the NLO-phores than those chains which are not packed as densely. Since densely packed chains exhibit less segmental mobility relative to unpacked chains, those NLO-phores that have been oriented by the electric field would be more likely to retain their orientation.

Support for the packing argument is found in experiments where the aging of the polymer films is erased by maintaining the films at temperatures well above the T_g for a period of time (at least 1 h) before the poling process is commenced. If the packing argument is correct, then the $\chi^{(2)}$ signal should be less stable and also exhibit a larger initial value. It can be seen in Figure 3 that indeed for both polymers the initial magnitude of the SHG signal is greater and the rate of decay for the signal is increased, particularly so in the case of **8c**. A small contribution to the magnitude of the drop may be caused by a third-order contribution; however, these effects usually occur over much shorter time scales and make a small percentage contribution.[16]

An interesting comparison is made between polymers **8d** (prepared from $\{\eta^5\text{-}C_5H_4CH_2O_2CC(CH_3)=CH_2\}Fe\{\eta^5\text{-}C_5H_4CH=C(CN)CO_2Et$ as previously reported[7d]) and **9**. Both are PMMA copolymers having essentially identical ferrocene NLO-phores; however, the NLO-phore in **8d** is decoupled from the polymer backbone through the ferrocenyl–Cp axis, a rotational mode not found in organic NLO-phores. Each system is heated to T_g or $T_g + 10$ °C (temperatures at which maximum $\chi^{(2)}$ is observed) and corona poled at that temperature for 10 min. Upon reaching ambient temperature, the field is removed and the decay of the SHG signal monitored. The decay of $\chi^{(2)}$ for the polymers is displayed in Figure 4. Polymer **8d** shows a faster relaxation at short times but plateaus to a stable signal at longer times. Once again, a biexponential equation is used to fit the data and is shown as the solid lines in Figure 4.

NLO-phore **5** represented an interesting opportunity to study the behavior of an organometallic NLO-phore possessing several sites for hydrogen bonding, a parameter we believe very important in controlling NLO-phore orientation. As can be seen in Figure 5, when subjected to positive corona poling, the NLO rapidly loses orientation much faster than the side-chain analog (*i.e.*, **8d**). However, negative corona poling leads to a much more stable SHG signal (Figure 5). This observation is consistent with a previous study on organic guest–host systems. The difference in decay rates may be attributed to the ability of the ITO glass substrate to inject charge. It is known

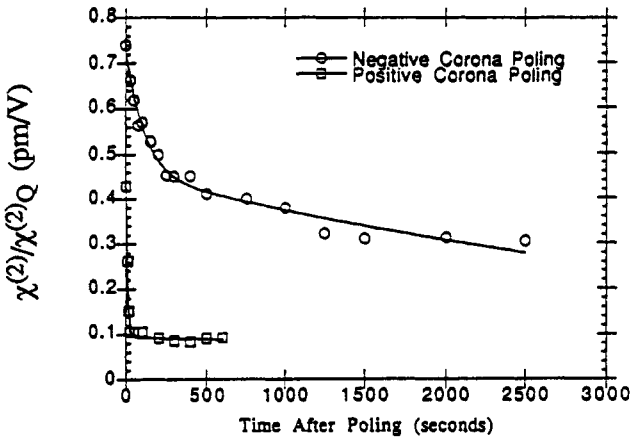

Figure 5. Decay of $\chi^{(2)}/\chi^{(2)}_Q$ following positive and negative corona poling of NLO-phore **5** in PMMA (5% by weight). The solid line indicates a biexponential fit for each case. For negative corona poling, the fitting parameters are $\theta_1 = 0.27$, $\tau_1 = 116$ s; $\theta_2 = 0.45$, $\tau_2 = 5103$ s and $\theta_1 = 0.34$, $\tau_1 = 10$ s; $\theta_2 = 0.09$, $\tau_2 = 14\,857$ s for positive corona poling.

that ITO glass can inject holes more readily than electrons. Charge transport and charge trapping are important issues when determining poling efficiencies.[15] Charge interaction with the redox-active ferrocene-based NLO-phore is also a possibility.

The last polymer tested in the study is the organometallic main-chain NLO system **10**. Previous ferrocene main-chain polymers prepared in our laboratory that possess a head-to-tail orientation and essentially identical NLO-phores have not displayed SHG activity after poling.[7b] We are gratified to report that polyurethane **10** does align at 150 °C by corona poling. The system shows reasonable stability for the SHG signal; however, concomitant decomposition of the NLO-phore (as evidenced by a color change from purple to red) during the cooling process leads to a severe underestimation of its true orientational stability. The fact that the present organometallic system, which is randomly oriented (in a head-to-tail sense), responds to poling illustrates that the additive effect of dipoles (a concept developed and discussed in NLO polymers by Katz *et al.*[19] and Williams *et al.*[20]) possible for head-to-tail oriented organometallic polymers must be matched by deleterious factors (chain packing, dipole–dipole interactions between polymer chains, ...) which make the latter unresponsive to poling.

Concluding Remarks. This study presents the first comprehensive experimental study probing the orientational and relaxation behavior of ferrocene-based organometallic NLO-phores in a polymer environment by the use of $\chi^{(2)}$ nonlinear optical spectroscopy. By varying the structure of the NLO-phore, we were able to determine that packing of the NLO-phore within the polymer matrix is very important and was shown to, in at least one case, dominate size considerations. Physical aging of the polymer films led to a reversible densification of the polymer matrix. The aged polymer films showed a greater resistance to alignment with a concomitant increase in the ability to retain NLO-phore alignment. These data are consistent with a packing argument. Erasure of the thermal history of aged films by heating prior to poling also supported the idea of tight packing through densification.

The inability of the WW equation to describe the decay data for the organometallic systems used in this investigation is consistent with certain previous studies of guest–host systems but does differ slightly from a more recent study of the organic guest–host and side-chain NLO polymers.[10] The present study used a slightly different protocol for sample preparation and data collection of the SHG signal. We believe this is in part responsible for the differences seen for the polymer relaxation data. In addition, and perhaps more importantly, the organometallic NLO-phores have very different shapes and relaxation mechanisms (*e.g.*, Fe–Cp rotation) available for reorientation. Studies are continuing involving the synthesis and evaluation of organometallic NLO polymers and supermacromolecular organometallic assemblies.

Experimental Section

Methods. All manipulations of compounds and solvents were carried out using standard Schlenk techniques. Solvents were degassed and purified by distillation under nitrogen from standard drying agents. Spectroscopic measurements utilized the following instrumentation: ^{1}H NMR, Varian XL 300; ^{13}C NMR, JEOL 270 (at 67.80 MHz). NMR chemical shifts are reported assigning the $CHCl_3$ (residual in $CDCl_3$) resonance at 7.25 ppm in ^{1}H and assigning the $CDCl_3$ resonance at 77.00 ppm in ^{13}C spectra. The (4-bromophenyl)acetonitrile, malononitrile, methacryloyl chloride, methyl methacrylate, and 1,6-diisocyanatohexane were all purchased from Aldrich Chemical and used as received. The 4-pyridylacetonitrile hydrochloride was suspended in ether, neutralized with $NaHCO_3$, and then dried under vacuum. GPC data were collected on a Varian 5000 HPLC employing a PL size-exclusion column (300 × 7.5 mm, 5-μm particle size). Molecular weight data are referenced relative to polystyrene standards. Polymer analyses were performed using Perkin-Elmer TGA 7 and DSC 7 systems. Elemental analyses were performed at Atlantic Microlab Inc., Norcross, GA.

SHG Measurements. A Continuum NY61-10 Q-switched Nd:YAG laser generated p-polarized light at 1.064 μm. The fundamental beam was split so that the sample and a y-cut quartz reference could be tested simultaneously, and lenses were used to vary the size and intensity of the laser beam impinging on the sample. Lenses were placed directly behind the sample and reference to focus the frequency-doubled light through infrared filters, insuring that only 532-nm light passed into the monochromator and photomultiplier tube (PMT). The PMT signal was sent to a gated integrator and boxcar averager. A Sparc IPC workstation was used to collect and store data. The sample was vertically mounted on a temperature-controlled copper block so that the laser beam struck the sample at a 68° angle relative to the normal of the sample. Samples were poled using a corona discharge generated by a tungsten needle across a 1-cm air gap. The corona current was limited to 3 μA to prevent damage to the sample.

Signal-to-noise ratios in the data are of the same size as the symbols in the figures, and data represent the average of between two and four independent samples. Temperature variations were controlled to within ±1 °C. $\chi^{(2)}$ values in the figures are shown relative to a quartz reference ($\chi^{(2)}/\chi^{(2)}_Q$). The initial values of $\chi^{(2)}$, relative to a quartz reference, are reproducible from sample to sample with errors of less than 5% (copolymer) to 10% (guest–host) (when corrected[18] for film thickness, etc.).

SHG Sample Preparation. The polymer samples were dissolved in spectrophotonic-grade chloroform (Mallinckrodt) to produce solutions with 10% polymer by weight. Solutions were filtered (5 μm) and then spun cast onto indium tin oxide (ITO) glass substrates. Film thicknesses varied from 2 to 6 (±0.5) μm, as measured by diamond stylus profilometry. Films were carefully dried to remove any excess solvent.

{η^5-$C_5H_4CH_2OH$}Fe{η^5-C_5H_4CH=C(CN)C_6H_4Br} (3a). A THF solution of lithium diisopropylamide (LDA) (3.80 mmol) was cannula transferred to a Schlenk flask containing a chilled (−78 °C) THF (10 mL) solution of (4-bromophenyl)acetonitrile. The mixture was allowed to react for 1 h at −78 °C and then cannula transferred to a flask containing a THF solution of **2** (1.02 g, 3.20 mmol) chilled to −78 °C. The cooling bath was removed and the mixture allowed to react with stirring overnight. The solvent was removed under reduced pressure, and the crude product was redissolved in a methanol solution and treated with

p-toluenesulfonic acid (30 mg) and stirred for 4 h. The solvent was removed under reduced pressure and the crude product subjected to column chromatography (2 × 15 cm) on alumina eluting with MeOH/CH_2Cl_2 (1/50, v/v) to afford **3a** (0.64 g, 58% yield): ^{1}H NMR ($CDCl_3$) δ 7.49 (m, 4 H, Ar), 7.35 (s, 1 H, =CH), 4.96 (t, J = 2 Hz, 2 H, Cp), 4.55 (t, J = 2 Hz, 2 H, Cp), 4.33 (d, J = 5.1 Hz, 2 H, CH_2OH), 4.29 (t, J = 2 Hz, 2 H, Cp), 4.23 (t, J = 2 Hz, 2 H, Cp), 4.17 (s, 1 H, OH); ^{13}C NMR ($CDCl_3$) δ 143.3 (=CH), 133.4 (Ar C), 132.1 (ArCH), 126.5 (Ar CH), 122.1 (Ar C), 118.6 (CN), 105.6 (=*C*(CN)), 89.3 (*ipso*-Cp), 72.1 (Cp CH), 70.4 (Cp CH), 69.9 (Cp CH), 69.4 (Cp CH), 60.1 (CH_2O); IR (CH_2Cl_2) $\nu_{C\equiv N}$ 2212 cm^{-1}; UV-vis (CH_2Cl_2) λ_{max} 494 nm. Anal. Calcd for $C_{20}H_{16}FeBrNO$: C, 56.91; H, 3.82; N, 3.32. Found: C, 57.09; H, 4.10; N, 3.12.

{η^5-$C_5H_4CH_2OH$}Fe{η^5-C_5H_4CH=C(CN)C_5H_4N} (3b). A THF LDA (4.63 mmol) solution was cannula transferred into a Schlenk flask containing a chilled (−78 °C) THF (10 mL) solution of 4-pyridylacetonitrile (0.46 g, 3.86 mmol). The mixture was allowed to react at −78 °C for 1 h and then cannula transferred to a Schlenk flask containing a THF solution of **2** (1.22 g, 3.86 mmol) chilled to −78 °C. The cooling bath was removed, and the mixture was allowed to warm to room temperature and remain stirring overnight. The solvent was removed under reduced pressure, and the crude product was redissolved in a methanol solution. To the solution was added TsOH (30 mg), and the mixture was stirred for 4 h at ambient temperature. The solvent was removed under reduced pressure and the crude product subjected to column chromatography (2 × 15 cm) on alumina. Gradient elution starting with CH_2Cl_2 and finishing with 2% MeOH/CH_2Cl_2 yielded pure **3b** (0.71 g, 54% yield): ^{1}H NMR ($CDCl_3$) δ 8.64 (m, 2 H, py), 7.62 (s, 1 H, =CH), 7.48 (m, 2 H, py), 5.02 (t, J = 2 Hz, 2 H, Cp) 4.63 (t, J = 2 Hz, 2 H, Cp), 4.33 (s, 2 H, CH_2O), 4.30 (t, J = 2 Hz, 2 H, Cp), 4.24 (t, J = 2 Hz, 2 H, Cp), 1.68 (br s, 1 H, OH); ^{13}C NMR ($CDCl_3$) δ 150.2 (py), 146.9 (=CH), 142.0 (*ipso*-py), 119.0 (py), 117.9 (C≡N), 103.5 (*C*(CN)-py), 89.9 (*ipso*-Cp), 73.0 (Cp CH), 71.0 (Cp CH), 70.0 (Cp CH), 69.6 (Cp CH), 59.7 (CH_2O); IR (CH_2Cl_2) $\nu_{C\equiv N}$ 2215 cm^{-1}; UV-vis (CH_2Cl_2) λ_{max} 510 nm (ϵ = 3.82 × 10^3). Anal. Calcd for $C_{19}H_{16}FeN_2O$: C, 66.30; H, 4.69; N, 8.14. Found: C, 66.21; H, 4.89; N, 7.89.

{η^5-$C_5H_4CH_2OH$}Fe{η^5-C_5H_4CH=C(CN)$_2$} (3c). A THF solution containing **1** (0.65 g, 2.7 mmol), malononitrile (0.21 g, 3.2 mmol), and K_2CO_3 (excess) was allowed to react for 2 h with stirring. The solvent was removed under reduced pressure, and the crude product was subjected to column chromatography. Elution with MeOH/CH_2Cl_2 (1/50, v/v) yielded pure **3c** (0.60 g, 75% yield): ^{1}H NMR ($CDCl_3$) δ 7.71 (s, 1 H, =CH), 4.98 (t, 2 H, J = 2 Hz, Cp CH), 4.83 (t, 2 H, J = 2 Hz, Cp CH), 4.35 (m, 4 H, Cp CH and CH_2), 4.30 (t, 2 H, J = 2 Hz, Cp CH), 1.62 (br s, 1 H, OH); ^{13}C NMR ($CDCl_3$) δ 163.2 (=CH), 115.0 (C≡N), 114.3 (C≡N), 90.7 (=*C*(CN)$_2$), 75.6 (Cp CH), 72.0 (Cp CH), 70.8 (Cp CH), 70.3 (Cp CH), 59.4 (CH_2); IR (CH_2Cl_2) $\nu_{C\equiv N}$ 2225 cm^{-1}; UV-vis (CH_2Cl_2) λ_{max} 530 nm (ϵ = 2.72 × 10^3). Anal. Calcd for $C_{15}H_{12}FeN_2O$: C, 61.68; H, 4.14; N, 9.59. Found: C, 61.18; H, 4.33; N, 9.48.

{η^5-$C_5H_4CH_2O_2CC(CH_3)$=CH_2}Fe{η^5-C_5H_4CH=C(CN)C_6H_4-Br} (4a). A Schlenk flask was charged with THF, **3a** (0.34 g, 0.98 mmol), Et_3N (0.21 mL, 1.47 mmol), and methacryloyl chloride (0.16 mL, 1.47 mmol) and allowed to react with stirring for 8 h at ambient temperature. The mixture was diluted with ether (100 mL) and the organic layer washed with water (2 × 100 mL) and brine (100 mL) and then dried over K_2CO_3. The solvent was removed under reduced pressure and the crude product subjected to column chromatography (2 × 10 cm) on alumina. Gradient elution starting with CH_2Cl_2 and finishing with MeOH/CH_2Cl_2 (1/99, v/v) gave a deep red band which was collected, and the solvents were removed under reduced pressure (0.32 g, 79%): ^{1}H NMR ($CDCl_3$) δ 7.49 (m, 4 H, Ar), 7.32 (s, 1 H, =CH), 6.08 (s, 1 H, =CH_2), 5.55 (s, 1 H, =CH_2), 4.96 (t, J = 2 Hz, 2 H, Cp), 4.90 (s, 2 H, CH_2OH), 4.54 (t, J = 2 Hz, 2 H, Cp), 4.34 (t, J = 2 Hz, 2 H, Cp), 4.24 (t, J = 2 Hz, 2 H, Cp), 1.92 (s, 3 H, CH_3); ^{13}C NMR ($CDCl_3$) δ 166.8 (CO_2), 142.9 (=CH), 136.0 (=*C*(CH_3)), 133.3 (Ar C), 132.0 (Ar CH), 126.5 (Ar CH), 125.6 (=CH_2), 122.1 (Ar C), 118.4 (CN), 106.0 (=*C*(CN)), 83.4 (*ipso*-Cp), 72.2 (Cp CH), 70.6 (Cp CH), 70.5 (Cp CH), 70.3 (Cp CH), 62.0 (CH_2O), 18.2 (CH_3); IR (CH_2Cl_2) $\nu_{C\equiv N}$ 2213 cm^{-1}; UV-vis (CH_2Cl_2) λ_{max} 494 nm (ϵ = 1.84 × 10^3). Anal. Calcd for $C_{24}H_{20}BrFeNO_2$: C, 58.8; H, 4.1; N, 2.9. Found: C, 58.6; H, 4.6; N, 2.6.

{η^5-$C_5H_4CH_2O_2CC(CH_3)$=CH_2}Fe{η^5-C_5H_4CH=C(CN)-C_5H_4N} (4b). In a manner similar to that of **4a**, complex **3b** (0.27 g, 0.78 mmol) was converted to **4b**. Purification was achieved using column chromatography (2 × 10 cm) on alumina, with gradient elution (CH_2Cl_2 → MeOH/CH_2Cl_2, 1/99, v/v) yielding a deep red band which was collected, and the solvents were removed under reduced pressure (0.25 g, 78%): ^{1}H NMR ($CDCl_3$) δ 8.63 (m, 2 H, py), 7.58 (s, 1 H, =CH), 7.49 (m, 2 H, py), 6.09 (s, 1 H, =CH_2), 5.55 (s, 1 H, =CH_2), 5.01 (t, J = 2 Hz, 2 H, Cp), 4.89 (s, 2 H, CH_2O), 4.63 (t, J = 2 Hz, 2 H, Cp), 4.36 (t, J = 2 Hz, 2 H, Cp), 4.27 (t, J = 2 Hz, 2 H, Cp), 1.92 (s, 3 H, CH_3); ^{13}C NMR ($CDCl_3$) δ 166.9 (CO_2), 150.5 (py), 146.2 (=CH), 141.7 (py), 136.0 (=*C*(CH_3)), 125.8 (=CH_2), 119.0 (py), 117.8 (CN), 104.5 (=*C*(CN)), 83.8 (*ipso*-Cp), 73.0 (Cp CH), 71.1 (Cp CH), 70.8 (Cp CH), 70.5 (Cp CH), 61.9 (CH_2O), 18.2 (CH_3); IR (CH_2Cl_2) $\nu_{C\equiv N}$ 2215 cm^{-1}; UV-vis (CH_2Cl_2) λ_{max} 508 nm (ϵ = 2.57 × 10^3). Anal. Calcd for $C_{23}H_{20}FeN_2O_2$: C, 67.01; H, 4.89; N, 6.79. Found: C, 65.90; H, 5.08; N, 6.39.

{η^5-$C_5H_4CH_2O_2CC(CH_3)$=CH_2}Fe{η^5-C_5H_4CH=C(CN)$_2$} (4c). A dichloromethane solution containing **3c** (0.48 g, 1.63 mmol), Et_3N (0.46 mL, 3.27 mmol), and methacryloyl chloride (0.35 mL, 3.27 mmol) was allowed to react with stirring at ambient temperature for 4 h. The mixture was diluted with ether (100 mL) and the organic layer washed with water (2 × 100 mL) and brine (100 mL) and then dried over K_2CO_3. The solvents were removed under reduced pressure and the crude product subjected to column chromatography (2 × 10 cm) on alumina. Gradient elution starting with CH_2Cl_2 and ending with MeOH/CH_2Cl_2 (1/99, v/v) yielded a purple band which was collected. The solvents were removed under reduced pressure to yield a purple solid (0.46 g, 79%): ^{1}H NMR ($CDCl_3$) δ 7.68 (s, 1 H, =CH), 6.14 (s, 1 H, =CH_2), 5.62 (s, 1 H, =CH_2), 4.97 (t, J = 2 Hz, 2 H, Cp), 4.86 (s, 2 H, CH_2O), 4.81 (t, J = 2 Hz, 2 H, Cp), 4.40 (t, J = 2 Hz, 2 H, Cp), 4.34 (t, J = 2 Hz, 2 H, Cp), 1.96 (s, 3 H, CH_3); ^{13}C NMR ($CDCl_3$) δ 166.9 (CH_2O_2C), 162.7 (=CH), 136.0 (=*C*Me), 114.7 (C≡N), 114.0 (C≡N), 85.2 (=*C*(CN)$_2$), 75.6 (Cp CH), 72.1 (Cp CH), 71.4 (Cp CH), 61.4 (CH_2O), 18.3 (CH_3); IR (CH_2Cl_2) $\nu_{C\equiv N}$ 2226 cm^{-1}; UV-vis (CH_2Cl_2) λ_{max} 526 nm (ϵ = 2.99 × 10^3). Anal. Calcd for $C_{19}H_{16}FeN_2O_2$: C, 63.36; H, 4.48; N, 7.78. Found: C, 63.10; H, 4.60; N, 7.50.

{$\eta^5C_5H_5$}Fe{η^5-C_5H_4CH=C(CN)$CO_2CH_2CH_2OH$} (5). A Schlenk flask was charged with THF (20 mL), ferrocenecarboxaldehyde (1.0 g, 4.7 mmol), $NCCH_2CO_2CH_2CH_2OH$ (2.5 g, 19 mmol), and an excess of K_2CO_3 and the mixture allowed to react at ambient temperature with stirring for 5 h. The mixture was filtered and the solvent removed under reduced pressure. The crude reaction mixture was subjected to column chromatography (3 × 15 cm) on alumina, eluting with CH_2Cl_2 to afford two purple bands. The slower moving band was collected, and solvents were removed to give **5** (0.97 g, 64%): ^{1}H NMR ($CDCl_3$) δ 8.22 (s, 1 H, CH=), 5.03 (t, J = 2 Hz, 2 H, Cp), 4.75 (t, J = 2 Hz, 2 H, Cp), 4.39 (t, J = 4.6 Hz, 2 H, CH_2), 4.27 (s, 5 H, Cp CH), 4.23 (t, J = 4.6 Hz, 2 H, CH_2); ^{13}C NMR ($CDCl_3$) δ 163.5 (CO_2), 159.4 (CH=CN), 116.9 (CN), 96.3 (=*C*(CN)CO_2), 74.3 (Cp CH), 71.8 (Cp CH), 70.6 (Cp CH), 67.5 (CH_2), 60.7 (CH_2); IR (CH_2Cl_2) $\nu_{C\equiv N}$ 2222 cm^{-1}; UV-vis (CH_2Cl_2) λ_{max} 522 nm (ϵ = 1.14 × 10^3). Anal. Calcd for $C_{16}H_{15}FeNO_3$: C, 62.21; H, 4.65; N, 4.31. Found: C, 62.61; H, 4.62; N, 4.67.

{η^5-C_5H_5}Fe{η^5-C_5H_4CH=C(CN)$CO_2CH_2CH_2O_2C$(C-H_3)=CH_2} (6). A Schlenk flask was charged with THF (10 mL), methacryloyl chloride (0.3 mL, 2.9 mmol), **5** (0.8 g, 2.4 mmol), and Et_3N (0.4 mL, 2.9 mmol) and the mixture allowed to react with stirring at ambient temperature for 6 h. The crude reaction mixture was diluted with ether (100 mL) and the organic layer washed with water (2 × 100 mL) and brine (100 mL) and then dried over K_2CO_3. The solvents were removed under reduced pressure, and the crude product was subjected to column chromatography (2 × 10 cm) on alumina, eluting with CH_2Cl_2. The purple band was collected, and the solvents were removed to afford pure **6** (0.68 g, 72%): ^{1}H NMR ($CDCl_3$) δ 8.19 (s, 1 H, =CH), 6.15 (s, 1 H, =CH_2), 5.60 (s, 1 H, =CH_2), 5.02 (t, J = 2 Hz, 2 H, Cp), 4.74 (t, J = 2 Hz, 2 H, Cp), 4.47 (m, 4 H, CH_2's), 4.26 (Cp), 1.95 (CH_3); ^{13}C NMR ($CDCl_3$) δ 163.1 (CO_2), 159.3 (=CH), 135.8 (=CH_2), 116.6 (CN), 96.4 (=*C*(CN)), 74.4 (Cp

CH), 71.9 (Cp CH), 70.7 (Cp), 63.4 (CH_2), 62.0 (CH_2), 18.3 (CH_3); IR (CH_2Cl_2) $\nu_{C\equiv N}$ 2223 cm^{-1}; UV-vis (CH_2Cl_2) λ_{max} 522 nm (ϵ = 3.43 × 10^3). Anal. Calcd for $C_{20}H_{19}FeNO_4$: C, 61.09; H, 4.87; N, 3.56. Found: C, 61.16; H, 5.04; N, 3.69.

{η^5-$C_5H_4CH_2OH$}Fe{η^5-$C_5H_4CH{=}C(CN)CO_2CH_2CH_2OH$} (7). A THF solution of $NCCH_2CO_2CH_2CH_2OH$ (2.5 g, 19 mmol) was cannula transferred into a Schlenk flask containing **1** (1.2 g, 4.9 mmol) and excess K_2CO_3. The mixture was allowed to react with stirring at ambient temperature for 6 h. The reaction mixture was filtered and the solvent removed under reduced pressure. The crude product was subjected to column chromatography (3 × 12 cm) on alumina using gradient elution (CH_2Cl_2 → MeOH/CH_2Cl_2, 1/50, v/v) affording **7** (0.94 g, 54%): ^1H NMR ($CDCl_3$) δ 8.21 (s, 1 H, =CH), 5.03 (t, J = 2 Hz, 2 H, Cp), 4.77 (t, J = 2 Hz, 2 H, Cp), 4.40 (t, J = 4.6 Hz, 2 H, CH_2), 4.33 (m, 4 H, Cp CH and CH_2), 4.25 (t, J = 2 Hz, 2 H, Cp), 3.93 (br s, 2 H, CH_2); ^{13}C NMR ($CDCl_3$) δ 163.4 (CO_2), 159.0 (=CH), 117.0 (CN), 96.4 (=C(CN)), 74.7 (Cp CH), 72.2 (Cp CH), 70.5 (Cp CH), 69.9 (Cp CH), 67.5 (CH_2), 60.6 (CH_2), 59.5 (CH_2); IR (CH_2Cl_2) $\nu_{C\equiv N}$ 2222 cm^{-1}; UV-vis (CH_2Cl_2) λ_{max} 522 nm (ϵ = 1.89 × 10^3). Anal. Calcd for $C_{17}H_{17}FeNO_4$: C, 57.49; H, 4.89; N, 3.94. Found: C, 56.80; H, 5.19; N, 4.59.

PMMA Copolymer 8a. A Schlenk flask was charged with benzene (3 mL), **4a** (0.20 g, 0.48 mmol), methyl methacrylate (1.03 mL, 9.6 mmol), and AIBN. The mixture was heated to reflux for 8 h and the solvent removed under reduced pressure. The polymer was redissolved in chloroform and precipitated in a methanol solution (0.64 g, 53%): ^1H NMR ($CDCl_3$) δ 7.50 (m, 4 H, Ar CH), 7.28 (s, 1 H, CH=C), 4.99 (t, J = 2 Hz, 2 H, Cp), 4.79 (s, 2 H, CH_2O), 4.57 (t, J = 2 Hz, 2 H, Cp), 4.34 (t, J = 2 Hz, 2 H, Cp), 4.23 (t, J = 2 Hz, 2 H, Cp), 3.59 (s, PMMA OCH_3), 1.91 (br s, PMMA CH_2), 1.83 (br s, 2 H, CH_2), 1.03 (s, PMMA CH_3), 0.85 (s, 3 H, CH_3). Anal. Calcd: N, 0.59. Found: N, 0.37.

PMMA Copolymer 8b. A Schlenk flask was charged with benzene (3 mL), **4b** (0.10 g, 0.25 mmol), methyl methacrylate (0.53 mL, 4.98 mmol), and AIBN. The mixture was heated to reflux for 8 h and the solvent removed under reduced pressure. The polymer was redissolved in chloroform and precipitated in a methanol solution (0.30 g, 49%): ^1H NMR ($CDCl_3$) δ 8.63 (m, 2 H, py), 7.59 (s, 1 H, =CH), 7.48 (m, 2 H, py), 5.01 (t, J = 2 Hz, 2 H, Cp), 4.75 (s, 2 H, CH_2), 4.62 (t, J = 2 Hz, 2 H, Cp), 4.32 (t, J = 2 Hz, 2 H, Cp), 4.26 (t, J = 2 Hz, 2 H, Cp), 3.58 (s, PMMA OCH_3), 1.87 (br s, PMMA CH_2), 1.79 (br s, 2 H, CH_2), 0.98 (s, PMMA CH_3), 0.86 (s, 3 H, CH_3). Anal. Calcd: N, 1.21. Found: N, 1.31.

PMMA Copolymer 8c. A Schlenk flask was charged with benzene (3 mL), **4c** (0.34 g, 0.95 mmol), methyl methacrylate (2.02 mL, 18.9 mmol), and AIBN. The mixture was heated to reflux for 8 h and the solvent removed under reduced pressure. The polymer was redissolved (~1.3 g did not dissolve) in chloroform and precipitated in methanol (0.55 g, 25%): ^1H NMR ($CDCl_3$) δ 7.73 (br s, 1 H, =CH), 4.99 (t, J = 2 Hz, 2 H, Cp), 4.84 (t, J = 2 Hz, 2 H, Cp), 4.70 (s, 2 H, CH_2), 4.37 (m, 4 H, Cp), 3.58 (s, PMMA OCH_3), 1.92 (br s, 2 H, PMMA CH_2), 1.79 (br s, 2 H, CH_2), 1.00 (s, PMMA CH_3), 0.82 (s, 3 H, CH_3). Anal. Calcd: N, 1.24. Found: N, 1.21.

PMMA Copolymer 9. A Schlenk flask was charged with **6** (0.34 g, 0.87 mmol), methyl methacrylate (1.9 mL, 17.4 mmol), AIBN (10 mg), and benzene (5 mL). The reaction was heated to 80 °C for 6 h. The resulting polymer was precipitated in methanol. The polymer was then redissolved in chloroform and precipitated in methanol (three times) to afford pure copolymer (1.2 g, 59%): ^1H NMR ($CDCl_3$) δ 8.21 (br s, 1 H, =CH), 5.06 (br s, 2 H, Cp), 4.76 (br s, 2 H, Cp), 4.45 (br s, 2 H, CH_2), 4.29 (s, 5 H, Cp), 4.25 (br s, 2 H CH_2), 3.58 (s, PMMA OCH_3), 1.88 (br s, PMMA CH_2), 1.79 (br s, 2 H, CH_2), 1.00 (s, PMMA CH_3), 0.82 (s, 3 H, OCH_3). Anal. Calcd: N, 0.55. Found: N, 0.61.

Polyurethane 10. A Schlenk flask containing **7** (0.24 g, 0.7 mmol), 1,6-diisocyanatohexane (0.1 mL, 0.7 mmol), and dioxane (3 mL) was heated to 100 °C for 10 h. The reaction mixture was poured into methanol to precipitate copolymer **10** as a purple solid (0.20 g, 55%): ^1H NMR ($CDCl_3$) δ 8.19 (s, 1 H, =CH), 5.28 (br s, 1 H, NH), 5.15 (br s, 1 H, NH), 5.01 (s, 2 H, Cp CH), 4.74 (s, 4 H, Cp CH and CH_2), 4.4–4.2 (m, 8 H, 2 CH_2's and 2 Cp CH's), 3.16 (br s, 4 H, NCH_2), 1.60 (br s, 2 H, CH_2), 1.49 (br s, 4 H, CH_2's), 1.32 (br s, 4 H, CH_2's); ^{13}C NMR ($CDCl_3$) δ 163.2 (CO_2), 159.14 (=CH), 156.3 (C=O(NH)), 156.1 (C=O(NH)), 116.6 (CN), 96.7 (=C(CN)), 85.8 (*ipso*-Cp), 74.8 (Cp CH), 74.6 (CH_2), 72.4 (Cp CH), 71.0 (Cp CH), 70.6 (Cp CH), 64.3 (CH_2O), 62.0 (CH_2O), 61.5 (CH_2O), 40.8, 29.7, 26.2 (CH_2's); IR (CH_2Cl_2) $\nu_{C\equiv N}$ 2221 cm^{-1}, $\nu_{C=O}$ 1756 and 1724 cm^{-1}; UV-vis (CH_2Cl_2) λ_{max} 520 nm (ϵ = 1.89 × 10^3). Anal. Calcd: N, 9.70. Found: N, 9.55.

Acknowledgment. M.E.W. expresses his gratitude for generous support of this research by the Office of Naval Research. H.S.L. acknowledges support for work by the Office of Naval Research and NSF through a PFF award.

References and Notes

(1) *Materials for Nonlinear Optics: Chemical Perspectives*; Marder, S. R., Sohn, J. E., Stucky, G. D., Eds.; ACS Symposium Series 455; American Chemical Society: Washington, DC, 1991; references cited therein.

(2) *Organic Materials for Nonlinear Optics*; Hann, R. A., Bloor, D., Eds.; Special Publication No. 69; Royal Society of Chemistry: London, 1989. *Organic Materials for Nonlinear Optics II*; Bloor, D., Ed.; Special Publication No. 91; Royal Society of Chemistry: London, 1991.

(3) Frazier, C. C.; Harvey, M. A.; Cockerman, M. P.; Hand, H. M.; Chauchard, E. A.; Lee, C. H. *J. Phys. Chem. Soc.* **1986**, *90*, 5703.

(4) Green, M. L. H.; Marder, S. R.; Thompson, M. E.; Bandy, J. A.; Bloor, D.; Kolinsky, P. V.; Jones, R. J. *Nature* **1987**, *330*, 360. Perry, J. W.; Stiegman, A. E.; Marder, S. E.; Coulter, D. R. *Organic Materials for Nonlinear Optics*; Hann, R. A., Bloor, D., Eds.; Special Publication No. 69; Royal Society of Chemistry: London, 1989. Coe, B. J.; Jones, C. J.; McCleverty, J. A.; Bloor, D.; Kolinsky, P. V.; Jones, R. J. *J. Chem. Soc., Chem. Commun.* **1989**, 1485. Marder, S. R.; Perry, J. W.; Tiemann, B. G. *Organometallics* **1991**, *10*, 1896.

(5) For a theoretical (SCF-LCAO MECI formalism) treatment of organometallic NLO materials, see: Kanis, D. R.; Ratner, M. A.; Marks, T. J. *J. Am. Chem. Soc.* **1990**, *112*, 8203.

(6) Rosenblum, M. *Chemistry of the Iron Group Metallocenes*; Wiley: New York, 1965. Harwood, J. W. *Industrial Applications of Organometallic Compounds*; Reinhold: New York, 1963. Johnson, J. C., Jr. *Metallocene Technology*; Noyes Data Corp.: Park Ridge, NJ, 1973. Neuse, E. W.; Woodhouse, J. R.; Montaudo, G.; Puglis, C. *Appl. Organomet. Chem.* **1988**, *2*, 53.

(7) (a) Wright, M. E.; Svejda, S. A. *Materials for Nonlinear Optics: Chemical Perspectives*; Marder, S. R., Sohn, J. E., Stucky, G. D., Eds.; ACS Symposium Series 455; American Chemical Society: Washington, DC, 1991; p 602. (b) Wright, M. E.; Toplikar, E. G. *Macromolecules* **1992**, *25*, 6050–6054. (c) Wright, M. E.; Sigman, M. S. *Macromolecules* **1992**, *25*, 6055–6059. (d) Wright, M. E.; Toplikar, E. G.; Kubin, R. F.; Seltzer, M. D. *Macromolecules* **1992**, *25*, 1838.

(8) A is the preexponential constant, y is the relaxation function, and τ is the characteristic relaxation time. β is a constant between zero and 1 that describes the deviation of the relaxation process from a single exponential: Hodge, I. M.; Berens, A. R. *Macromolecules* **1982**, *15*, 762.

(9) Hampsch, H. L.; Yang, J.; Wong, G. K.; Torkelson, J. M. *Macromolecules* **1990**, *23*, 3640. Hampsch, H. L.; Yang, J.; Wong, G. K.; Torkelson, J. M. *Macromolecules* **1988**, *21*, 526. Hampsch, H. L.; Yang, J.; Wong, G. K.; Torkelson, J. M. *Polym. Commun.* **1989**, *30*, 40. Hampsch, H. L.; Torkelson, J. M.; Bethke, S. J.; Grubb, S. G. *J. Appl. Phys.* **1990**, *67*, 1037.

(10) Walsh, C. A.; Burland, D. M.; Lee, V. Y.; Miller, R. D.; Smith, B. A.; Twieg, R. J.; Volksen, W. *Macromolecules* **1993**, *26*, 3720.

(11) Wright, M. E. *Organometallics* **1990**, *9*, 853.

(12) Wright, M. E.; Toplikar, E. G. *Contemporary Topics in Polymer Science, Volume 7*; Riffle, J., Ed.; Plenum Publishing Co.: New York, 1992; p 285.

(13) Hampsch, H. L.; Yang, J.; Wong, G. K.; Torkelson, J. M. *Macromolecules* **1990**, *23*, 3648. Lackritz, H. S.; Torkelson, J. M. Polymer Physics of Poled Polymers for Second Order Nonlindear Optics. In *Molecular Optoelectronics: Materials, Physics, and Devices*, Zyss, J., Ed.; Academic Press: New York, 1993; Chapter 8, in press.

(14) Shen, Y. R. *Principles of Nonlinear Optics*; John Wiley & Sons: New York, 1984.

(15) This is an important consideration but one that is difficult to quantify as discussed in ref 13.

(16) Boyd, G. T. *J. Opt. Soc. Am. B* **1989**, *6*, 685. Dhinojwala, A.; Wong, G. K.; Torkelson, J. M. *Macromolecules* **1993**, *26*, 5943. Dhinojwala, A.; Wong, G. K.; Torkelson, J. M. *Macromolecules*, in press.

(17) Walsh, C. A.; Buland, D. M.; Lee, V. Y.; Miller, R. D.; Smith, B. A.; Tweig, R. J.; Volksen, W. *Macromolecules* **1993**, *26*, 3720. Eich, M.; Sen, A.; Looser, H.; Yoon, D. Y.; Bjorklund, G. C.; Tweig, R.; Swalen, J. D. *Proc. SPIE* **1988**, *971*, 128. Eich, M.; Sen, A.; Looser, H.; Bjorklund, G. C.; Swalen, J. D.; Tweig, R.; Yoon, D. Y. *J. Appl. Phys.* **1989**, *66*, 2559.

(18) Singer, K. D. *Proc. SPIE* **1991**, *1560*, 469. Singer, K. D.; Lalama, S. J.; Sohn, J. E. *Proc. SPIE* **1985**, *578*, 130. Singer, K. D.; Kuyzk, M. G.; Holland, W. R.; Sohn, J. E.; Lalama, S. J.; Cornizzoli, R. B.; Katz, H. E.; Schilling, M. L. *Appl. Phys. Lett.* **1988**, *53*, 1800. Singer, K. D.; Kuzyk, M. G.; Sohn, J. E. *J. Opt. Soc. Am. B* **1987**, *4*, 968.

(19) Katz, H. E.; Schilling, M. L.; Fang, T.; Holland, W. R.; King, L.; Gordon, H. *Macromolecules* **1991**, *24*, 1201 and references cited therein.

(20) Ulman, A.; Wiland, C. S.; Köhler, W.; Robello, D. R.; Williams, D. J.; Handley, L. *J. Am. Chem. Soc.* **1990**, *112*, 7083 and references cited therein.